RECENT DEVELOPMENTS IN THE APPLICATION OF RF SUPERCONDUCTIVITY TO HIGH-BRIGHTNESS AND HIGH-GRADIENT ION BEAM ACCELERATORS

J. R. Delayen, C.L. Bohn, W.L. Kennedy, G.L. Nichols, C.T. Roche, L. Sagalovsky
Engineering Physics Division
Argonne National Laboratory
9700 South Cass Avenue, Argonne, Illinois 60439

ABSTRACT

A development program is underway to apply rf superconductivity to the design of continuous-wave (cw) linear accelerators for high-brightness ion beams. Since the last workshop, considerable progress has been made both experimentally and theoretically toward this application. Recent tests of niobium resonators for ion acceleration have yielded average accelerating gradients as high as 18 MV/m. In an experiment with a radio-frequency quadrupole geometry, niobium was found to sustain cw peak surface electric fields as high as 128 MV/m over large (10 cm^2) surface areas. Theoretical studies of beam impingement and cumulative beam breakup have also yielded encouraging results. Consequently, a section of superconducting resonators and focusing elements has been designed for tests with high-current deuteron beams. In addition, considerable data pertaining to the rf properties of high-T_c superconductors has been collected at rf-field amplitudes and frequencies of interest in connection with accelerator operation. This paper summarizes the recent progress and identifies current and future work in the areas of accelerator technology and superconducting materials which will build upon it.

1. INTRODUCTION

The technology of radio-frequency superconductivity (RFSC) offers a number of advantages for the production of high-current, high-brightness ion beams.[1] A fundamental advantage is that thermal management of the accelerator is accomplished inherently due to the very low wall losses in the constituent superconducting resonators. This has been exploited in the construction of a number of superconducting linacs designed to produce either high-energy electron beams or low-current, high quality ion beams for scientific applications.[2,3] These linacs are economical to operate, and they run cw (a duty factor of 100%) virtually unattended for long periods. Another key advantage is that superconducting low-velocity linacs are comprised of relatively short, independently phased accelerating cavities. This adds reliability because if a fraction of the cavities are off-line, the linac can still be operated with full performance by increasing and rephasing the fields in the remaining cavities.

Our recent efforts have focused on extending the existing technology base for low-brightness, low-frequency ion accelerators into that required for high-brightness, high-frequency linacs. We are also studying advanced superconducting materials for accelerator applications, an effort which includes the measurement of the rf properties of high-T_c superconductors.

In this paper, we first enumerate the major development work areas leading to high-brightness superconducting ion linacs. We then summarize recent experimental results in niobium resonator development and recent theoretical results concerning beam impingement, cumulative beam breakup, and current limits in superconducting RFQs. We follow this with a brief description of the design of a superconducting section for high-current ion-beam tests. Recent experimental results concerning the rf performance of high-T_c superconductors are then summarized. We conclude with a synopsis of future work motivated by these results.

2. MAJOR DEVELOPMENT WORK AREAS

2.1. Resonator Geometry

Superconducting accelerators for new applications often require new cavity designs. Designs which are good for normal-conducting cavities generally are poor for superconducting cavities. Because of their low power dissipation, superconducting cavities do not need to be designed to maximize the shunt impedance, and new designs which would be inefficient for normal-conducting cavities can be explored. Successful superconducting cavities operate with a minimum amount of electron loading in the form of multipactoring (resonant electron emission) and/or field emission (nonresonant electron emission). Electron loading is difficult to predict accurately, but it is known to be a function both of cavity geometry and conditions at the surface of the superconductor.

Our designs of niobium resonators for the acceleration of high-brightness ion beams incorporate coaxial resonant lines with the beam traversing the high-voltage region. This approach was found to be successful in the development of existing slow-wave structures at lower frequencies.[3] These resonators are 2-gap structures and therefore can efficiently accelerate a broad range of particle mass and velocity. Recent results for these structures are summarized in Section 3 below.

2.2. Beam Impingement

There is little experimental data on the amount of beam impingement a superconducting cavity can sustain without going normal, but it should not exceed a few watts per cavity. This can translate to as little as a few particles per million hitting the resonator. In turn, the radial profile of the beam halo can be important in this context. However, beam impingement can be mitigated by designing superconducting resonators with large apertures and/or beam scrapers. An example calculation of beam impingement is given in Section 4.1 below.

2.3. Focusing

Space-charge effects in high-current beams will have to be countered with strong and frequent focusing. Because a superconducting resonator must go through its transition on cool-down in the absence of ambient magnetic fields, permanent magnets cannot be located inside the

drift tubes. Instead, superconducting magnets located outside the cavities must be used, and these would be turned on after cool-down. Experiments indicate that superconducting cavities can maintain their rf properties in the presence of high dc magnetic fields, which means the focusing elements can be located very close to the cavities with modest shielding.[4]

2.4. Beam Instabilities

Because the modes of superconducting cavities have high unloaded quality factors (Q), beam instabilities due to the excitation of higher-order modes must be considered in conjunction with accelerator designs. In ion linacs, multi-pass beam breakup is not an issue. The designs under consideration for superconducting linacs involve the use of short, completely decoupled cavities. This leaves cumulative beam breakup as the dominant transverse instability, and this problem is considered in Section 4.2 below.

2.5. Beam Loading, Control

When accelerating beams of several tens of milliamps, the power supplied to the beam will be several orders of magnitude higher than that dissipated in the superconducting cavities, so the cavities will be heavily beam loaded. The process of critically coupling to these beam-loaded structures for the efficient transfer of power to the beam will lead to low external Qs. The relatively large bandwidth associated with these low external Qs will simplify beam control by eliminating the effects of variations in the resonant frequency due to ambient vibrations. A potentially deleterious consequence of heavy beam loading may occur if a cavity were to go normal. Then the rf fields generated by the beam itself would lead to large wall losses and, in turn, high consumption of cryogen. To counter this possibility, fast frequency tuners would be needed to shift rapidly the resonant frequencies and reduce the coupling between the cavity and beam.

2.6. Materials

Niobium technology is still far from achieving its full theoretical potential due to the presence of field emission. Current research in the treatment of niobium cavities is therefore focused on reducing field emission.[5] Niobium-alloy technology is still in its infancy,[6,7] and high-T_c superconductors are not yet ready for application in accelerating cavities.[8] Niobium alloys offer the possibility of operating at higher surface magnetic fields. Their higher transition temperatures may also improve thermal stability and reduce sensitivity to beam impingement. The same remarks apply likewise to high-T_c superconductors, which offer the additional potential of operation with liquid nitrogen, a consideration which leads to higher efficiency.[9] In view of their advantages, both niobium alloys and high-T_c superconductors should be pursued, but niobium remains the material of choice for near-term applications. Our measurements of the rf properties of high-T_c superconductors are summarized in Section 6 below.

3. NIOBIUM RESONATOR DEVELOPMENT

3.1. Accelerating Cavities

3.1.1 Coaxial quarter-wave geometry

The first superconducting accelerating cavity to be fabricated as part of our development effort was a 400 MHz coaxial quarter-wave structure optimized for particle velocity 0.15c. As is pictured in Figure 1, it consisted of an inner conductor fabricated from 0.16-cm-thick sheet niobium and an outer conductor consisting of sheet niobium which had been explosively bonded to copper. The cavity was operated in vacuum. Cooling was accomplished by filling the inner conductor with liquid helium and placing the outer conductor in thermal contact with a helium reservoir. This enabled cooling of the outer conductor by thermal conduction through the copper.

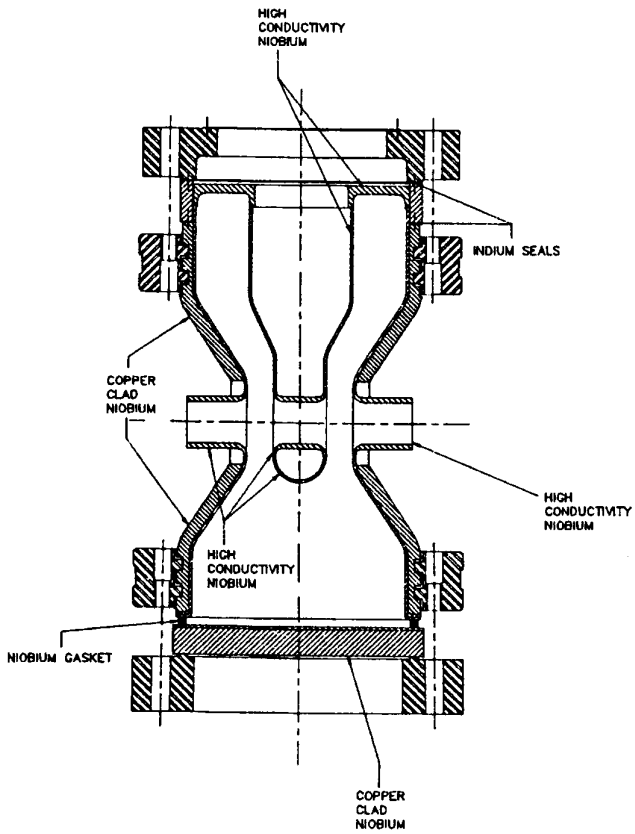

Figure 1. 400 MHz coaxial quarter-wave resonator; β_0=0.15.

The axial electric field profile was measured by pulling a 6.4-mm-diameter brass bead along the beam axis.[10] Within the measurement error, the shape of the profile agreed with that calculated assuming an electrostatic field distribution.[11] The average (wall-to-wall) accelerating gradient calculated from this profile was E_{acc} = (10.2 MV/m)/$J^{1/2}$. This cavity can efficiently accelerate ions of energy in the range 4-40 MeV/amu. The properties of the resonator are summarized in Table 1.

At the frequencies typically encountered in particle accelerators, the surface resistance (R_s) and quality factor (Q) of the resonator are strongly influenced by the condition of the cavity's interior surface. Among the contaminants which will degrade resonator performance are adsorbed hydrocarbons and non-superconducting metallic inclusions. Precautions were taken to minimize surface abrasion during the fabrication process and to treat the cavity's inner surface to remove contamination.

Table 1. Properties of the coaxial quarter-wave resonator.

Frequency	400 MHz
β_o	0.15
Energy gain[a)]	63.5 kV
Peak surface E field[a),b)]	3.2 MV/m
Peak surface B field[a),b)]	58 G
Energy content[a)]	9.6 mJ
Geometrical factor QR_s	38.3 Ω

[a)]at an accelerating field of 1 MV/m.
[b)]calculated from Ref. 11.

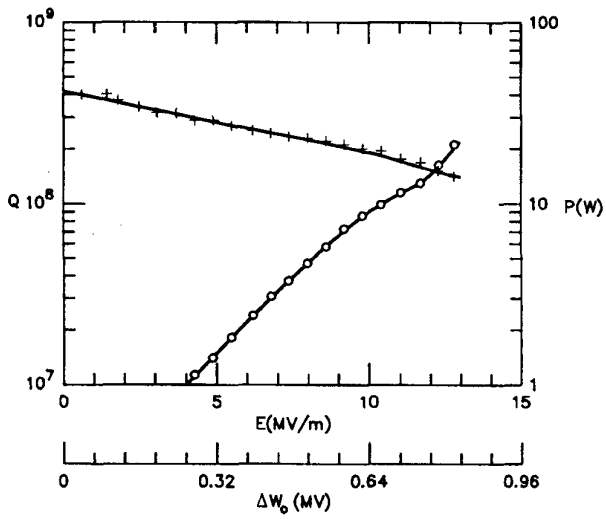

Figure 2. Q-curve (+) and power dissipation (o) for the 400 MHz quarter wave resonator.

The surface treatment of the center conductor began with electropolishing in a 17:3 solution of sulfuric acid and hydrofluoric acid respectively. This was followed by annealing in a $4x10^{-7}$ torr vacuum for approximately 13 hours at 1200 C and an additional electropolish. Afterwards, the piece was annealed a second time and welded to the outer conductor. A final treatment of the niobium surfaces of the whole resonator was done to remove surface imperfections generated during the welding of the inner and outer conductors. A chemical polish using a 2:1:1 solution of phosphoric acid, nitric acid, and hydrofluoric acid, respectively, was performed. Additional details concerning fabrication and niobium surface preparation of this cavity are available elsewhere.[12,13]

To provide rf power, a variable coupler was installed at the beam entrance aperture of the resonator. An rf pickup probe was installed at the beam exit aperture. A phase-locked loop was used to counter the effects of eigenfrequency noise due to ambient vibrations and microphonics. During the experiment, rf power was critically coupled to the cavity. Several multipacting levels appeared as the power input to the cavity was increased. These levels processed out very rapidly, however, to the point where no remaining multipacting levels were observed. The processing time was approximately one hour, most of which was spent in adjusting the phase-locked loop after each change in power input.

As shown in Figure 2, Q varied from $4.1x10^8$ at low rf field amplitude to $1.4x10^8$ at the highest field achieved. An average cw accelerating gradient of 12.9 MV/m was achieved with

21 W of rf power input to the cavity. This corresponds to an energy gain of 0.820 MV per unit charge. The associated peak surface electric and magnetic fields were approximately 41 MV/m and 750 G, respectively. A thermal instability probably unrelated to electron loading prevented operation at higher gradients.

3.1.2 Coaxial half-wave geometry

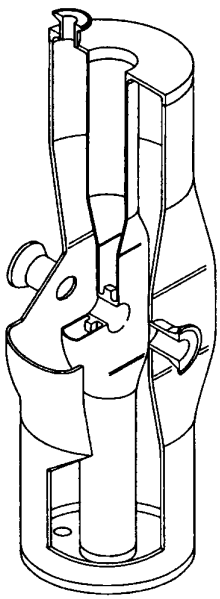

Figure 3. 355 MHz coaxial half-wave resonator; β_0=0.12.

Subsequently, a 355 MHz coaxial half-wave sheet niobium structure optimized for particle velocity 0.12c was fabricated. As is pictured in Figure 3, it consisted of an inner conductor fabricated from 0.16-cm-thick sheet niobium and an outer conductor fabricated from 0.32-cm-thick sheet niobium. During testing, the cavity was cooled by immersing it in liquid helium.

The axial electric-field profile, which was measured by pulling a 6.4-mm-diameter brass bead along the beam axis, is similar to that of the quarter-wave resonator. The average (wall-to-wall) accelerating gradient calculated from this profile was E_{acc} = (9.1 MV/m)/$J^{1/2}$. The properties of the resonator are summarized in Table 2.

Table 2. Properties of the coaxial half-wave resonator.

Frequency	355 MHz
β_o	0.12
Energy gain[a)]	70.0 kV
Peak surface E field[a),b)]	3.2 MV/m
Peak surface B field[a),b)]	52 G
Energy content[a)]	12 mJ
Geometrical factor QR_s	53.3 Ω

[a)]at an accelerating gradient of 1 MV/m.
[b)]calculated from Ref. 11.

The chemical polishing procedure consisted of filling the niobium cavity with a 2:1:1 solution of phosphoric acid, nitric acid, and hydrofluoric acid, respectively. This was followed by rinsing the piece in a 5% solution of H_2O_2 to remove insoluble niobium salts and then rinsing with deionized water of semiconductor purity. After the final chemical polish the resonator was

stored in a deionized water bath for approximately 48 hrs. prior to mounting the rf pickup and drive coupling loops. The final step prior to rf testing of the cavity was to clean ultrasonically the structure in a high-purity methanol bath. A high-temperature anneal of this cavity was never performed because no oven of suitable size was available. Additional details concerning fabrication and niobium surface preparation of this cavity are available elsewhere.[13]

To provide rf power, a fixed coupling loop was installed at the port of one of the end plates of the resonator. An rf pickup loop was installed at the port of the other end plate. The cryostat was surrounded by mu-metal to shield the resonator from ambient magnetic fields. A phase-locked loop was used to counter the effects of eigenfrequency noise due to ambient vibrations and microphonics.

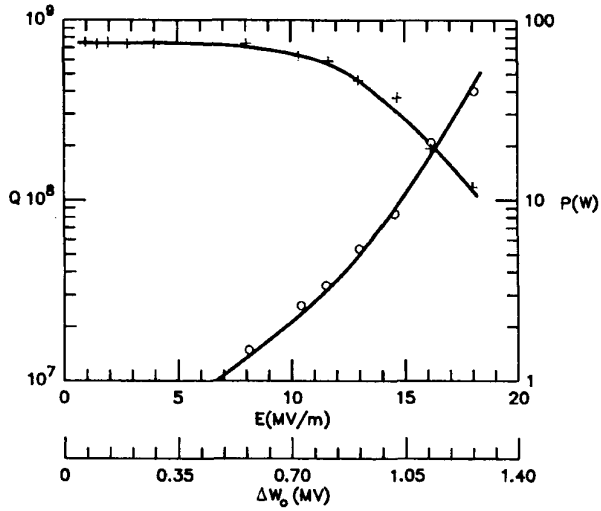

Figure 4. Q-curve (+) and power dissipation (o) for the 355 MHz coaxial-half-wave resonator.

Early in the experiment, several multipacting levels appeared which processed out almost immediately. A Q-curve was measured by monitoring the forward, reflected and pickup powers. An average cw accelerating gradient of 18.0 MV/m was then achieved with 40 W of rf power input to the cavity. As shown in Figure 4, Q varied from 7.7×10^8 at low rf field amplitude to 1.2×10^8 at the highest field achieved. This would provide an energy gain of 1.26 MV per unit charge. The associated peak surface electric and magnetic fields were approximately 58 MV/m and 936 G, respectively. X-ray radiation was monitored with a detector located external to the cryostat. Electron loading in the form of field emission was present, and x-rays were therefore generated. By measuring the bremmstrahlung from the most energetic electrons, the average accelerating gradient was calculated and found to agree with the gradient calculated from the forward and reflected powers at the cavity.

3.1.3 Spoke resonator geometry

The 2-gap spoke resonator geometry shown in Figure 5 is being investigated for use at frequencies which are higher than can be achieved with practical resonator designs incorporating coaxial geometries. In the fundamental accelerating mode, the inner conductor acts as a half-wavelength resonant line. This geometry is easier to fabricate reliably than is the coaxial half-wave geometry because there are fewer welds, and the critical welds located in the vicinity of high rf surface magnetic fields are accessible for visual inspection and polishing during the manufacturing process. The geometry can also be straightforwardly extended to multigap designs which should provide larger real-estate gradients than would be achievable with 2-gap structures.

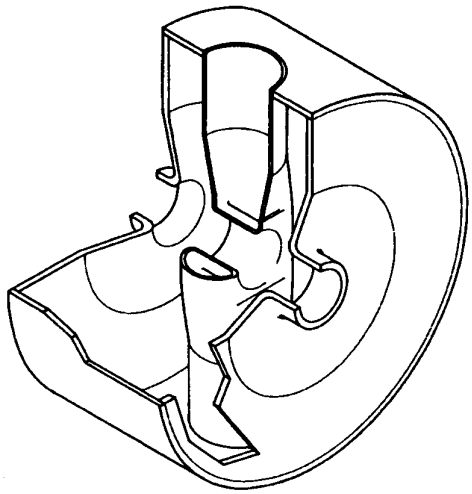

Figure 5. Conceptual design of a 2-gap spoke resonator.

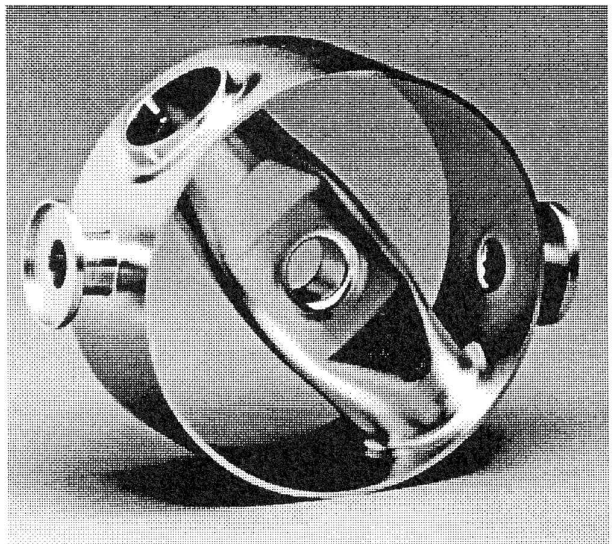

Figure 6. 850 MHz, β=0.28, 2-gap spoke resonator prior to the welding of the end plates.

A 2-gap, 850 MHz spoke resonator optimized for ß=0.28 has been fabricated from high-purity niobium and is undergoing initial tests. During the first series of tests, cw accelerating fields of 11 MV/m were obtained with very little Q degradation due to field emission. The resonator will be further tested after additional chemical polishing of the surface. A photo of this resonator just prior to final welding of the end plates appears in Figure 6. As part of the design process, the 3D cavity code MAFIA[14] was used to calculate the fields in this cavity and thereby specify its dimensions.

3.2. RF quadrupole geometry (Collaboration with Physics Division)

As the first step toward establishing a range of parameters for the design of superconducting radio-frequency quadrupole (RFQ) accelerating structures, a "voltage platform", shown in Figure 7, was constructed to determine, for a realistic vane geometry, the field gradients which could be expected in the cw operation of a superconducting RFQ.[15] The drift tubes of an existing niobium split-ring resonator were modified to support the four-finger structure shown in Figure 8 which consists of 7-cm-long niobium vanes. The aperture diameter is 6 mm, the vane edge radius is 2 mm, and the minimum distance between vanes of opposite voltage is 3.1 mm.

As indicated in Figure 9, the low-field Q was approximately constant. It was primarily determined by resistive losses associated with the rf surface magnetic field. Above 100 MV/m the losses increased rapidly with a corresponding decrease in Q. CW fields of 128 MV/m could be sustained over a surface area of order 10 cm^2 and were limited by the inefficient cooling of the vanes. Higher fields could be achieved in pulsed operation by gradually reducing the duty factor; 210 MV/m could be maintained for times in excess of 1 msec. The increased losses at

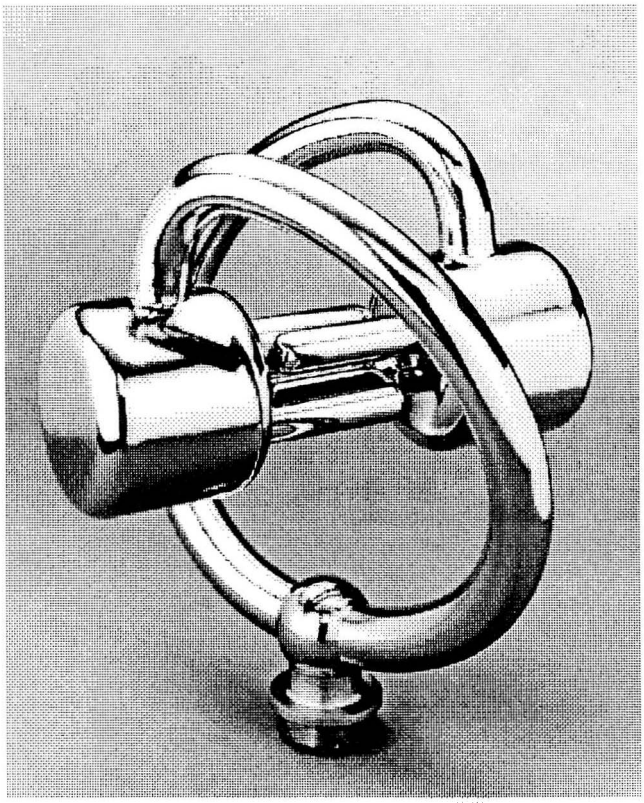

Figure 7. Niobium split-ring assembly with RFQ vanes prior to being welded to the outer housing.

high fields were due to electron loading in the form of field emission. The power input at 115 MV/m was 0.9 W per cm of rf quadrupole length.

This initial superconducting RFQ device has operated at fields a factor of three higher than have been reported for cw operation of normally-conducting RFQ devices.[16] The present results suggest that RFSC may appreciably extend the range of options for RFQ design.[17] For example, the use of RFQ vanes with deep modulations to provide simultaneous acceleration and strong focusing may enable very high real-estate gradients (tens of MV/m) to be achieved. If so, correspondingly compact linacs could be developed for the acceleration of high-current beams provided beam impingement can be held to a manageable level.

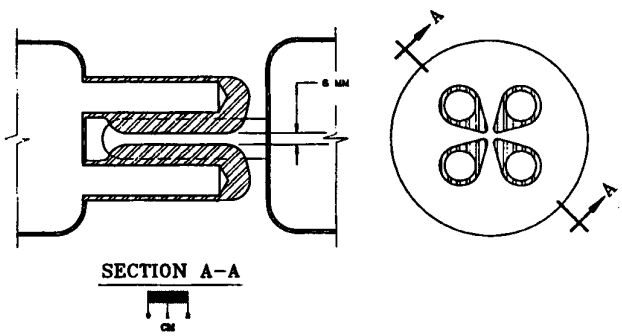

Figure 8. Four-finger geometry. The fingers are hollow to accept liquid helium.

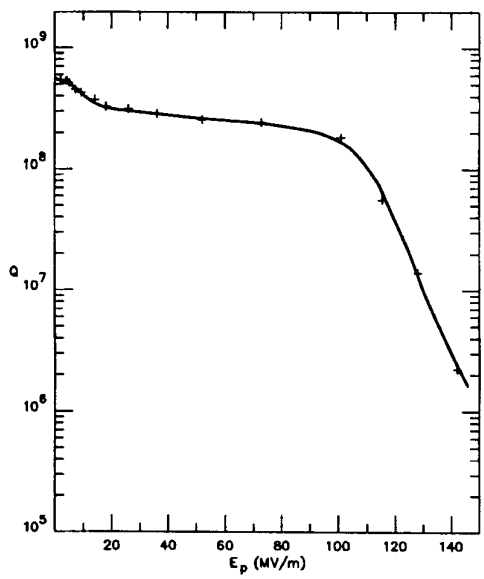

Figure 9. Q-curve for four-finger RFQ geometry.

4. THEORETICAL CONSIDERATIONS

4.1. Beam impingement

This example calculationof beam impingement in a superconducting linac includes an analysis of heat transport both in the resonator wall and at the interface between the resonator wall and the cryogen. The model incorporates a worst-case assumption that the ions will deposit their total kinetic energy (taken to be 200 MeV) at the niobium-vacuum interface. The heat-transport problem is approximated as one-dimensional heat flow across a plane. The cryogen is assumed to be liquid helium at 4.2 K (He I).

The heat-transport problem is dominated by the interface between the resonator wall and the liquid helium. To maximize the heat flux while minimizing the temperature difference at the interface, it is necessary to operate in the nucleate-boiling regime and to avoid film boiling. This will limit the rate of heat removal to 1 W/cm^2 and the temperature difference between the wall and bath to 1 K.[18] This assumption of heat transfer to static helium is conservative. Cooling can be done by forced flow of liquid helium, and higher heat transfer between the niobium and the helium would be possible. Adhering to the static-case assumption and assuming that the accelerating structure is fabricated from RRR=250 niobium, which has thermal conductivity $\sim$1 W/cm-K at 5.2 K,[19] the temperature rise at the niobium-vacuum interface is calculated to be $\sim$0.2 K. Since niobium has T_c=9.2K, this temperature increase would not present a serious problem for a cavity operating at 4.2 K.

The rate of heat removal restricts the amount of beam which can be permitted to impinge on a resonator. A two-dimensional Gaussian beam of 200 MeV H^- ions with σ_{rms}=0.6 mm and 100 mA current is assumed. Given this beam and a 1 W/cm^2 heat flux, the minimum diameter of the drift tube aperture required to avoid thermal runaway would be 6.7 mm if the beam were perfectly centered. By comparison, typical superconducting resonators, for example the accelerating cavities described above, have apertures of order 25 mm. We therefore conclude that, with these large apertures in the constituent resonators, beam impingement in these structures will be too low to result in a thermal management problem. Moreover, both beam scrapers and focusing elements can be used between the resonators to reduce beam impingement further.

4.2. Cumulative beam breakup

The cumulative beam breakup instability is caused by interaction between the beam and deflecting higher-order modes in the accelerating cavities. The most problematic deflecting modes have longitudinal electric-field components which are zero along the beam axis and change sign across the axis. The initial bunch of a misaligned beam excites the deflecting mode in the initial cavity which deflects trailing bunches. The deflected bunches then couple more strongly to the deflecting mode in the next cavity causing further deflection of trailing bunches, etc.

An analytic model of cumulative beam breakup has been developed which is applicable to both low-velocity ion and high-energy electron linacs.[20-23] A "continuum approximation" is made

in which the transverse kicks in momentum imparted by the cavities are smoothed over the length of the linac. The resulting equation of transverse motion is then solved via the WKBJ method.

The solution can be decomposed into the transient behavior and the steady-state behavior of the beam. Depending on the ratio of the deflecting-mode frequency to the accelerating-mode frequency, and on the strength of the focusing elements, the steady-state behavior may or may not be stable. In an unstable situation, the steady-state transverse displacement of the beam grows exponentially as the beam progresses down the linac. This growth can be greatly accentuated if the deflecting-mode frequency is in resonance with the accelerating-mode frequency. By applying sufficiently strong focusing along the linac, the steady-state behavior can be stabilized.

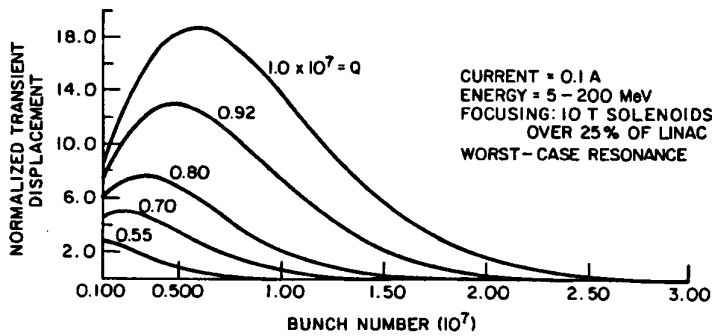

Figure 10. Normalized transient displacement x_M/x_0 vs. bunch number M at the last cavity of the full linac (see text). Curves correspond to different values of Q of the deflecting mode.

We investigated cumulative beam breakup in two superconducting linacs comprised of 352 MHz coaxial half-wave resonators supplying a 4.5 MV/m real-estate gradient. The first is the five-cavity section described in Section 5 below which is being designed for testing with a deuterium beam of energy 7.5 MeV and current 80 mA. It was modelled pessimistically using a tightly bunched, unfocused coasting beam which was misaligned at the entrance aperture of the accelerator. Under conditions of a worst-case beam-cavity resonance, an estimated maximum Q of 2×10^7 for the deflecting mode assures steady-state growth no larger than approximately twice the initial beam offset. The second is a 100 mA linac from 5 MeV to 200 MeV. It was modelled using a nonrelativistic, tightly bunched beam which was misaligned at the entrance aperture of the accelerator. The linac was assumed to provide a linear acceleration profile and strong solenoidal focusing (10 T solenoids over 25% of the linac). As shown in Figure 10, the transverse behavior of the beam was found to be very sensitive to the Q of the deflecting mode. Under conditions of a worst-case beam-cavity resonance, an estimated maximum Q of 5.5×10^6 for the deflecting mode assures transient growth no larger than approximately twice the initial beam offset.

In summary, a maximum Q of order 5×10^6 for the deflecting modes in the constituent resonators of these superconducting linacs should suppress the cumulative beam breakup instability under worst-case conditions. In actual operation, the external Q of the accelerating mode due to the rf coupling loops is expected to be considerably less than this. The rf coupling would therefore probably also provide an external $Q < 10^6$ for the deflecting mode and thereby control beam breakup.

We have also generalized the theory to include the effects of finite bunch length and arbitrary current distribution within each bunch.[21,22] Bunches of short, but finite, length were found always to exacerbate BBU relative to delta-function bunches. Bunches of finite length may be severely distorted by the deflecting modes, even in circumstances which would be stable were the bunches to have zero length. In each case, however, focusing can be used as a cure.

As an example, the formalism was used to calculate the steady-state cumulative beam breakup of a coasting beam consisting of uniform bunches. A simulation corresponding to an unfocused beam with parameters which are plausible for a superconducting linac is presented in Figure 11a. These results show that portions of each bunch can be deflected to transverse displacements exceeding the initial displacement even though the bunch centroids are deflected toward the axis. However, as shown in Figure 11b, focusing can be used to suppress bunch distortion.

These calculations leave unchanged the basic conclusion of the aforementioned calculations based on delta-function bunches, but they indicate that cumulative BBU can lead to transverse emittance growth through distortion of the bunches.

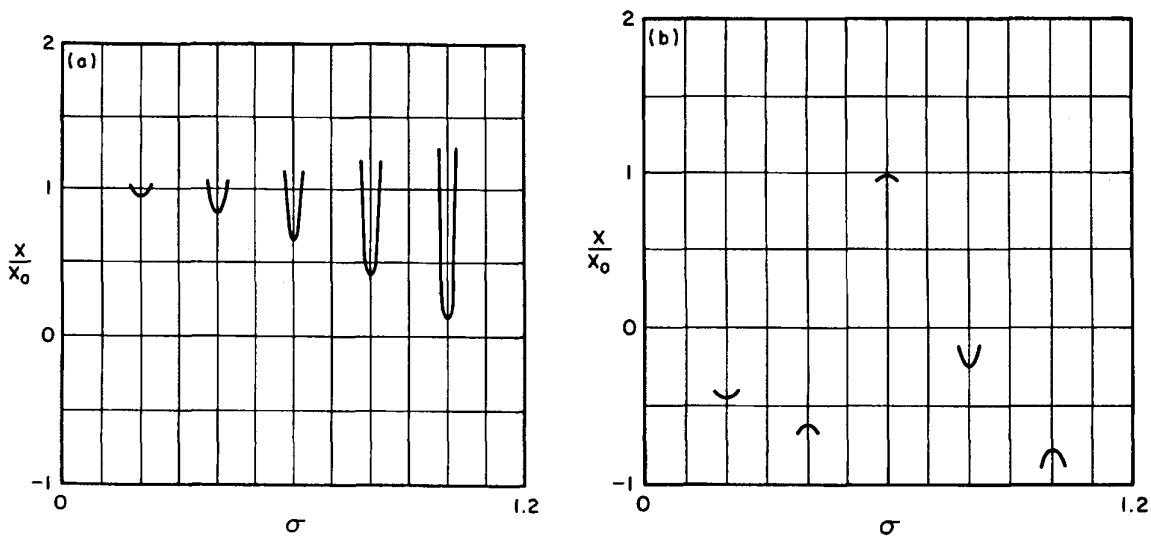

Fig. 11. Example plots of steady-state bunch displacement and shape vs. position σ along a linac with (a) no focusing and (b) focusing. Transverse displacement, plotted as the ordinate, is normalized with respect to the initial displacement. $\sigma = 0$ denotes the entrance to the linac, and $\sigma = 1$ denotes the exit.

4.3. Current limits in superconducting RFQs

The experimental data taken with the RFQ geometry mentioned earlier suggest that RFSC may appreciably extend the range of options for an RFQ design. In particular, it may be

possible to achieve cw beam currents in a SCRFQ which are unattainable with normal-conducting structures due to sparking limits and/or power dissipation in the walls of the structure.

We have initiated analytical and simulation studies to calculate current limits for SCRFQs which differ from the conventional RFQs in two main respects: very high cw electric fields can be sustained on the superconducting surface, and the tolerance to beam impingement is unknown but probably less than for normal-conducting RFQs (NCRFQ).

The overall current limit is taken to be the value at which the transverse and longitudinal limits are equal. The upper bound I_{max} is defined as the current of a uniformly charged ellipsoid at which the maximum extent of the beam envelope is equal to the minimum aperture inside the RFQ.[24] The actual current limit I_{lim} in an SCRFQ is reached when only a small fraction of the particles hit the vanes, thereby constituting a thermal load. It is characterized by a "halo impact parameter" ρ: $I_{lim} = \rho I_{max}$. We estimate a lower bound on the current limit by computing ρ for a Gaussian distribution, generally regarded as the worst-case scenario for a current density inside linacs, under different assumptions for the beam-spill tolerance.

Preliminary estimates suggest that I_{max} for SCRFQs is at least a factor of five larger than for NCRFQs. Our pessimistic estimate gives $\rho \approx 1/3$, indicating a current limit in SCRFQs which is about twice that in NCRFQs. Further work is in progress, and is focused on refining this estimate via the computation of beam halo by analytic modelling and N-body calculations.

5. SUPERCONDUCTING SECTION DEVELOPMENT

The preliminary design of a section consisting of five niobium spoke resonators interspersed with superconducting quadrupole focusing elements has been formulated. A conceptual drawing of the section appears in Figure 12. Once constructed, the section will be installed at the exit aperture of CWDD, a 352 MHz cryo-copper accelerator which is projected to provide a deuterium beam of energy 7.5 MeV and current up to 80 mA. The section will be used principally for experiments concerning beam dynamics in superconducting high-current ion linacs as well as for the development of diagnostic tools and beam-control systems for use with these linacs. Issues associated with focusing and beam loading/control will be explored. Experiments are projected to include measurements of: beam impingement and beam breakup, stability with respect to beam modulation in both amplitude and phase, the influence of gas condensation on long-term operation, effects of failure of individual linac elements on the beam dynamics, and assorted beam-physics experiments which take advantage of the independent operation of the linac components.

The cavities are designed to operate at 352 MHz and assumed to provide average accelerating gradients of 10 MV/m, an assumption which is based on the existing experimental data. Both 2-gap and 3-gap spoke resonators are currently being considered. The spoke-resonator geometry is favored over the coaxial half-wave geometry due to its relative ease of fabrication. The cavities will be cooled either by immersing them in liquid helium, or by surrounding them with jackets filled with liquid helium. The former approach has the advantage of simplicity but the disadvantage of requiring many hermetic seals. The latter approach

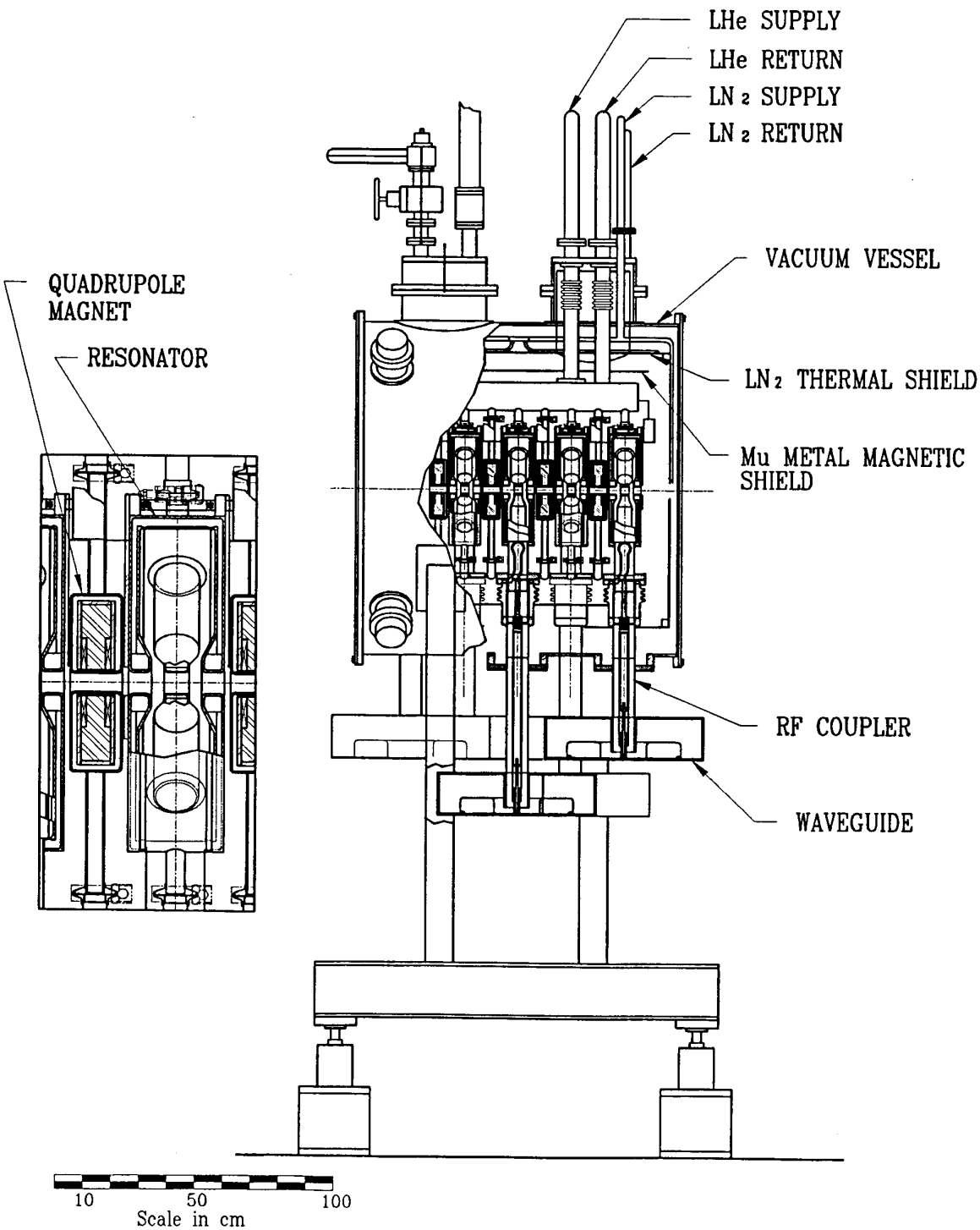

Figure 12. Conceptual drawing of a high-current superconducting test section designed for a 7.5 MeV deuterium beam. It comprises 5 accelerating cavities operating at 352 MHz; focusing is provided by superconducting quadrupoles located between the cavities.

(depicted in Figure 12) has the advantage of avoiding the need for hermetic seals but the disadvantage of a more complicated cavity design. Superconducting quadrupole magnets were chosen over solenoids as focusing elements because , at higher beam energy, they would provide a more compact design which, in turn, would result in higher real-estate gradients for the linac.

Insofar as possible, the section is being designed to provide current-independent performance while preserving emittance. Preliminary beamlines were generated using the TRACE3D code, modified to model independently phased multigap cavities. The TRACE3D results were then substantiated with N-body simulations using a modified version of PARMILA. The 3-gap structures would provide a real-estate gradient of order 25% larger than the 2-gap structures; however, 3-gap spoke resonators have not yet been fabricated.

6. RF PERFORMANCE OF HIGH-T_c SUPERCONDUCTORS

To be useful in accelerating cavities, high-T_c superconductors must have sufficiently low surface resistances (a few tens of micro-ohms) at high rf surface magnetic fields (a few hundred gauss). They also must take the form of films on substrates of high thermal conductivity, because the high-T_c superconductors themselves have poor thermal conductivity. We have constructed and used several apparatuses for measurements of rf surface resistances at frequencies from 0.15 to 40 GHz and rf surface magnetic fields as high as 640 gauss.[8]

A wide variety of polycrystalline films on silver and dielectric substrates spanning an enormous range of materials and fabrication techniques have been measured using a suitably designed coaxial quarter-wave cavity.[25] As shown in Figure 13, the qualitative behavior of R_s versus B_{rf} for polycrystalline high-T_c films on silver substrates was found to be identical for each material: R_s increases monotonically with field amplitude through a transition region characterized by a strong field dependence, and then saturates at high field at a value of a few percent of the normal-state surface resistance just above T_c. Regarding applications in accelerating cavities, our data indicate that at low rf fields, sufficiently low surface resistances are achieved, but at high rf fields (e.g., $\geq$ 30 gauss) the surface resistances are too large by a factor typically $\sim$100. This is a signature of the polycrystalline nature of the films and does not reflect their intrinsic properties. For example, R_s of epitaxial films on dielectric substrates degraded at high fields, but were substantially better than R_s of the polycrystalline films at high fields. Nevertheless, it is clear that the degradation in surface resistance of large-area high-T_c superconductors needs to be mitigated by a suitable process of materials engineering before they can be of use in accelerating cavities.

7. SUMMARY AND FUTURE WORK

Recent developments in rf superconductivity have been very promising. Niobium resonators fabricated for high-brightness ion acceleration have yielded cw average accelerating gradients as high as 18 MV/m. In an experiment with a superconducting RFQ geometry, cw surface electric fields as high as 128 MV/m were sustained over surface areas of order 10 cm^2.

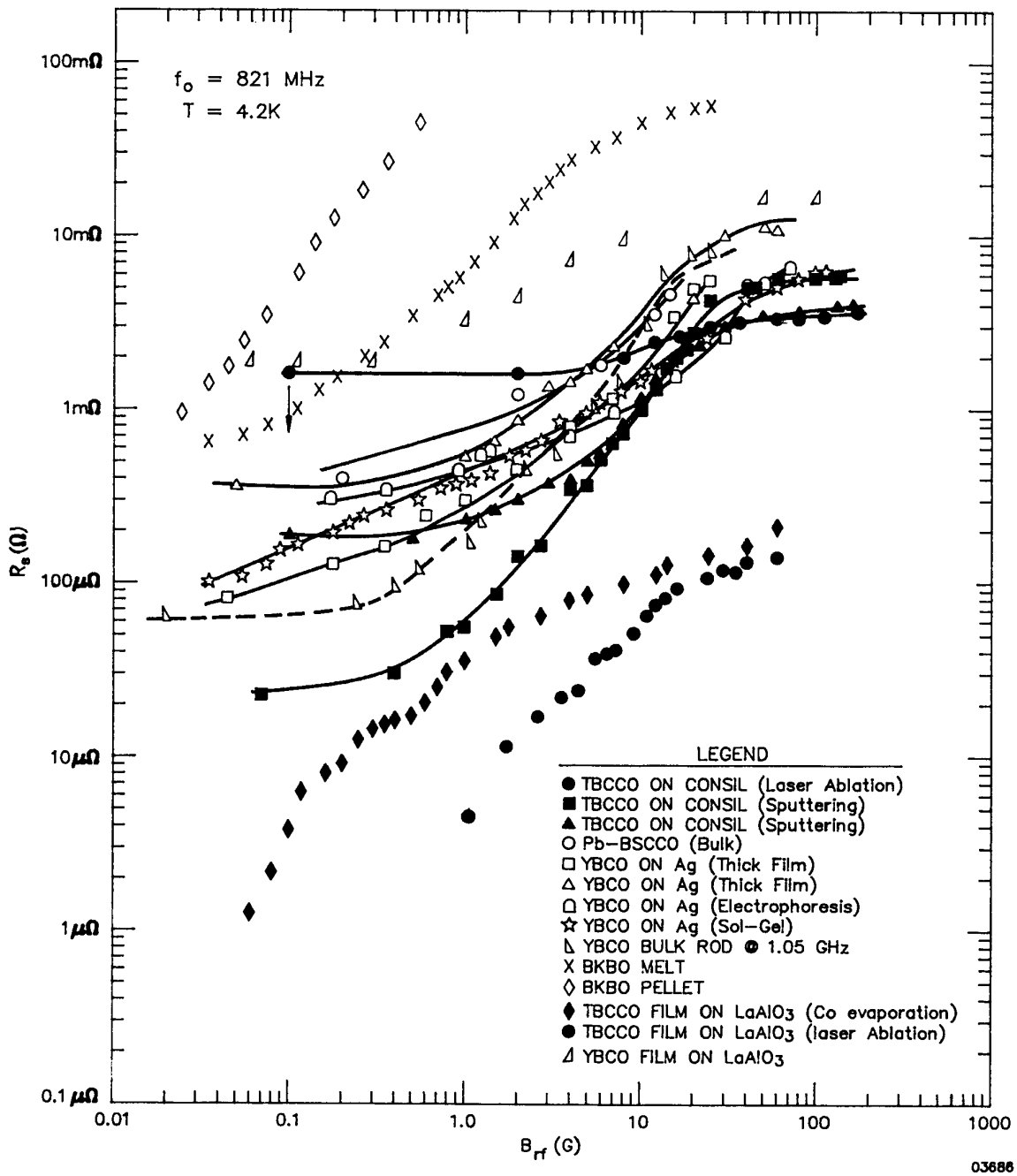

Figure 13. Surface resistance vs rf magnetic field for a variety of high-T_c samples. The data were taken at 820 MHz and 4.2 K.

Analyses of beam impingement and cumulative beam breakup in superconducting linacs comprised of decoupled, independently phased cavities were likewise encouraging.

These results point to the intrinsic potential of niobium to provide large accelerating gradients. They also show that RFSC technology may provide an extended range of options for RFQ design, including the possibility of developing RFQs for the acceleration of high currents at high real-estate gradients. The design of superconducting RFQs has been initiated, and we plan to begin shortly the construction of superconducting RFQs for tests with beam.

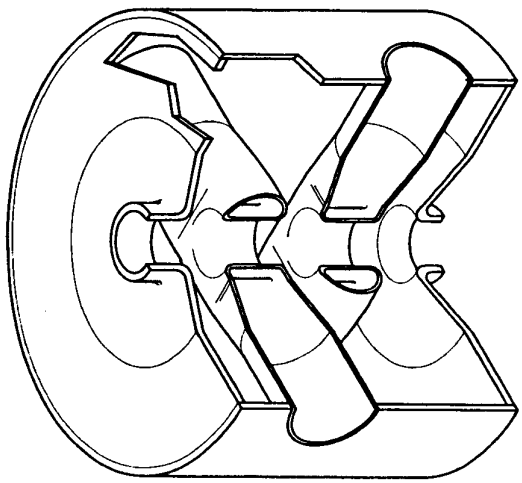

Figure 14. Conceptual design of a 3-gap spoke resonator.

In addition to the construction and testing of a superconducting section, future work will include the development of superconducting cavities for high-brightness ion linacs operating at higher frequencies. Work in progress includes the fabrication of a 3-gap, 850 MHz, β_0=0.28, spoke resonator like that shown in Figure 14.

The design of superconducting RFQs has been initiated, and construction of superconducting RFQs for tests both without and with beam is slated to begin shortly. Plans include tests of a superconducting cavity using the high-current beam from Chalk River Nuclear Laboratory's RFQ-1250, and tests of superconducting RFQs using the high-current beam from Culham Laboratory's Ion Source Test Stand.

Materials-related research will continue to be directed toward improving the performance of both low-T_c and high-T_c superconductors. Improvements in the thermal conductivity of niobium is especially helpful in this context because it simplifies the cooling of the cavities. The development of advanced low-T_c materials such as niobium films and niobium alloys will also be initiated in view of the additional benefits these materials can provide.

The rf surface resistances of a wide variety of high-T_c films have been measured as a function of rf magnetic field. Though the rf properties of high-T_c superconductors have been improving, to date no high-T_c film has been produced on a large-area metallic substrate which performs adequately for use in accelerating cavities.

7. ACKNOWLEDGEMENTS

This work was performed under the auspices of the U.S. Department of Energy and supported by the U.S. Army Strategic Defense Command and the Office of Naval Research. We are grateful to C. Batson for his assistance in all phases of the experiments discussed herein.

REFERENCES

1. J.R. Delayen, "Superconducting Accelerating Structures for High-Current Ion Beams", *Proc. 1988 Linear Accelerator Conference*, CEBAF-Report-89-001, pp. 199-201, 1989.

2. K.W. Shepard, "Status of Superconducting rf Cavity Development", *Proc. 1989 Particle Accelerator Conference*, Chicago, IL, Mar. 1989, pp. 1764-1768.

3. J.R. Delayen, "Low-Velocity Superconducting Accelerating Structures", *Proc. 4th Workshop on rf Superconductivity*, KEK, Tsukuba, Japan, Aug. 1989, pp. 249-265.

4. R. Benaroya, K.W. Shepard, "Superconducting RF Cavity in a DC Magnetic Field", *Rev. Sci. Instrum.*, **59**, 2100-2101, (1988).

5. Q.S. Shu, W. Hartung, A. Leibovich, J. Kirchgessner, D. Moffat, R. Noer, H. Padamsee, D. Rubin, and J. Sears, "Reducing Field Emission in Superconducting rf Cavities for the Next Generation of Particle Accelerators", *IEEE Trans. Magnetics*, **27**, 1935-1939, 1991.

6. M. Peiniger, G. Müller, H. Piel, and P. Thüns, "Nb_3Sn for Superconducting Accelerators at 4.2 K", *Proc. European Particle Accelerator Conference*, World Scientific Publishing Co., Singapore, 1989.

7. P. Fabbricatore, P. Fernandes, G.C. Gualco, F. Merlo, R. Musenich, and R. Parodi, "Study of Niobium Nitrides for Superconducting rf Cavities", *J. Appl. Phys.*, **66**, pp. 5944-5949, 1989.

8. J.R. Delayen, C.L. Bohn, and C.T. Roche, "Measurements of the rf Surface Resistance of High-T_c Superconductors at High rf Fields", *J. Supercon.*, **3**, pp. 243-250, 1990.

9. H. Padamsee, "Superconducting Structures for Electron Accelerators", *J. Supercon.*, **1**, pp. 377-393, 1988.

10. L.C. Maier, Jr. and J.C. Slater, "Field Strength Measurements in Resonant Cavities", *J. Appl. Phys.*, **23**, pp. 68-77, 1952.

11. J.R. Delayen, "Design of Low Velocity Superconducting Accelerating Structures Using Quarter-Wavelength Resonant Lines", *Nucl. Instrum. and Meth.*, **A259**, pp. 341-357, 1987.

12. J.R. Delayen, C.L. Bohn, and C.T. Roche, "A Superconducting Quarter-Wave Resonator for High-Brightness Ion Beam Acceleration", *Nucl. Instrum. and Meth.*, **A295**, pp. 1-4, 1990.

13. J.R. Delayen, C.L. Bohn, and C.T. Roche, "Niobium Resonator Development for High-Brightness Ion Beam Acceleration", *IEEE Trans. Magnetics*, **27**, 1924-1927, 1991.

14. T. Weiland, DESY.

15. J.R. Delayen and K.W. Shepard, "Tests of a Superconducting rf Quadrupole Device", *Appl. Phys. Lett.*, **57**, pp. 514-516, 1990.

16. S.O. Schriber, "Factors Limiting the Operation of Structures Under High Gradient", *Proc. 1986 Linear Accelerator Conference*, SLAC Report 303, pp. 591-596, 1986.

17. A. Schempp, H. Deitinghoff, J.R. Delayen, and K.W. Shepard, "Design and Application Possibilities of Superconducting Radio-Frequency Quadrupoles", *Proc. 1990 Linear Accelerator Conference*, Los Alamos Report **LA-12004-C**, 79-81, 1990.

18. D.N. Lyon, "Boiling Heat Transfer and Peak Nucleate Boiling Fluxes in Saturated Liquid Helium Between the λ and Critical Temperatures", *Adv. Cryo. Eng.*, **10**, pp. 371-379, 1965.

19. H. Elias and W. Weingarten, "Construction and Test of a Device for Thermal Conductivity Measurements Between 2 K and 10 K", *CERN/EF/RF 82-8*, Nov. 1982.

20. C.L. Bohn and J.R. Delayen, "Cumulative Beam Breakup in Radiofrequency Linacs", *Proc. 1990 Linear Accelerator Conference*, Los Alamos Report **LA-12004-C**, 306-308, 1990.

21. J.R. Delayen and C.L. Bohn, "Beam Breakup with Longitudinal Halo", *Proc. 1991 Particle Accelerator Conference*.

22. C.L. Bohn and J.R. Delayen, "Beam Breakup with Finite Bunch Length", *Proc. 1991 Particle Accelerator Conference*.

23. C.L. Bohn and J.R. Delayen, "Cumulative Beam Breakup in Linear Accelerators with Periodic Beam Current", (in preparation).

24. T.P. Wangler, "Space-Charge Limits in Linear Accelerators", Los Alamos Report **LA-8388**, 1981.

25. J.R. Delayen, C.L. Bohn, and C.T. Roche, "Apparatus for Measurement of Surface Resistance versus rf Magnetic Field of High-T_c Superconductors", *Rev. Sci. Instrum.*, **61**, pp. 2207-2210, 1990.